EVOLUTION & DEVELOPMENT 11:5, 590–602 (2009)
DOI: 10.1111/j.1525-142X.2009.00365.x

Developmental constraints revealed by co-variation within and among molar rows in two murine rodents

Sabrina Renaud,[a,*] Sophie Pantalacci,[b] Jean-Pierre Quéré,[c] Vincent Laudet,[b] and Jean-Christophe Auffray[d]

[a]Paléoenvironnements et Paléobiosphère, UMR 5125, CNRS, Université Lyon 1, Campus de la Doua, 69622 Villeurbanne, France
[b]Molecular Zoology Team, Institut de Génomique Fonctionnelle de Lyon, Université Lyon 1, CNRS, INRA, Ecole Normale Supérieure de Lyon, 46 allée d'Italie, 69364 Lyon Cedex 07, France
[c]INRA, Centre de Biologie et Gestion des Populations, UMR 1062, Campus International de Baillarguet, 34988 Montferrier/Lez cedex, France
[d]Institut des Sciences de l'Evolution, UMR 5554, Université Montpellier 2, CNRS, 34095 Montpellier Cedex, France
*Author for correspondence (email: sabrina.renaud@univ-lyon1.fr)

SUMMARY Morphological integration corresponds to interdependency between characters that can arise from several causes. Proximal causes of integration include that different phenotypic features may share common genetic sets and/or interact during their development. Ultimate causes may be the prolonged effect of selection favoring integration of functionally interacting characters, achieved by the molding of these proximal causes. Strong and direct interactions among successive teeth of a molar row are predicted by genetic and developmental evidences. Functional constraints related to occlusion, however, should have selected more strongly for a morphological integration of occluding teeth and a corresponding evolution of the underlying developmental and genetic pathways. To investigate how these predictions match the patterns of phenotypic integration, we studied the co-variation among the six molars of the murine molar row, focusing on two populations of house mice (*Mus musculus domesticus*) and wood mice (*Apodemus sylvaticus*).

The size and shape of the three upper and lower molars were quantified and compared. Our results evidenced similar patterns in both species, size being more integrated than shape among all the teeth, and both size and shape co-varying strongly between adjacent teeth, but also between occluding teeth. Strong co-variation within each molar row is in agreement with developmental models showing a cascade influence of the first molar on the subsequent molars. In contrast, the strong co-variation between molars of the occluding tooth rows confirms that functional constraints molded patterns of integration and probably the underlying developmental pathways despite the low level of direct developmental interactions occurring among molar rows. These patterns of co-variation are furthermore conserved between the house mouse and the wood mouse that diverged >10 Ma, suggesting that they may constitute long-running constraints to the diversification of the murine rodent dentition.

INTRODUCTION

A variety of traits were involved in mammalian evolution that enabled these animals to adopt a great variety of feeding strategies, leading to new and more complex diets, and the exploitation of new food niches. This key evolution for the success of mammals included evolution in jaw and tongue musculature, specialization of stomach and intestine, and within the dentition, the formation of cusped teeth and their occlusion between the complex tooth rows. Occluding teeth enable food to be ground and chewed more effectively and thus represent a pivotal point in the evolution leading to mammals. The increasing complexity of tooth crown shape might have participated to enable the maintenance of a high metabolic rate and therefore endothermy (Kemp 1982). It obviously constituted a constant selective constraint throughout the evolution of lineages: whatever the change in one tooth, other teeth had to change in consequence to maintain functional occlusion. Such a case exemplifies that individual phenotypic characters and genes are not free to evolve independently but that they evolve within the larger context of the organism in which they occur (Cheverud 1982). This interdependency of characters is referred as "morphological integration" (Olson and Miller 1958). Integration can arise from several causes. Proximal causes of integration include that different phenotypic features may share common genetic sets and/or interact during their development; ultimate causes may be the prolonged effect of selection favoring integration of functionally interacting characters, achieved by the molding of these proximal causes (Olson and Miller 1958; Klingenberg

© 2009 Wiley Periodicals, Inc.

2008). The degree of interdependence among morphological characters is directly related to the degree of integration, and can be measured by the intensity of statistical association in the phenotype (Cheverud 1982). What patterns of integration can actually be expected among teeth, based on our knowledge about the different possible sources of integration?

From the genetic point of view, making teeth probably requires a set of similar genes whatever the tooth considered (Tucker and Sharpe 2004; Zhang et al. 2005), but the achievement of very different morphologies in the upper and lower molar rows also implies some genetic independence. Integration among occluding molar rows is supported by the fact that among the numerous genes required for normal mouse molar development, only two are known to have a strict jaw-specific requirement: *Dlx1* and *Dlx2* (Qiu et al. 1997) and *Activin-βA* (Ferguson et al. 1998). In contrast, a relative independence between occluding tooth rows is supported by a QTL analysis (Shimizu et al. 2004) showing that among seven QTL found to influence molar size and shape, three were specific of the upper molar row, three specific of the lower row, and only one QTL was common between the two rows.

From a developmental point of view, a strong integration is expected within a tooth row. Experimental evidences suggest that within a developmental field, for instance the molar field, the first teeth to develop influences the successive ones in cascade (Kavanagh et al. 2007). Furthermore adjacent teeth should directly interact in accordance with the "neighborhood rule" (Van Valen 1970), corresponding to obvious mutual influence due to spatial contiguity.

Finally, from a functional point of view, morphological integration among occluding teeth is expected to be the most important if selection actually molded genetic networks and developmental pathways.

These predictions can be tested by investigating the patterns of morphological integration observed within and among molar rows. Most of these experimental data have been gathered using the laboratory mouse, making the mouse and its allies the adequate natural model to compare experimental predictions and empirical measures of morphological integration. The mouse and other murine rodents (Murinae or Old World rats and mice) have a derived molar row devoid of premolars, and consisting of three molars only, making them a simplified model to test the predictions regarding integration among teeth.

Morphological integration can be estimated by co-variation among characters. Focusing on co-variation at the intrapopulation level should reveal patterns produced by genetic and developmental pathways, being them molded by selection for functional occlusion or not. The robust evaluation of co-variation requires a good sampling of the considered population. Two extensively wild-trapped populations of murine rodents offered an adequate sampling: one belonging to the house mouse (*Mus musculus domesticus*), the other sampling the wood mouse (*Apodemus sylvaticus*). These two species belong to well-differentiated clades (Murini and Apodemini, respectively) that have diverged >10 Ma (Lecompte et al. 2008). They thus offer the opportunity to evaluate the patterns of co-variation within each species and to further consider if these patterns have been conserved across the murine radiation.

On these two populations, we quantified both size and shape of the three upper and three lower molars (Fig. 1) using an outline analysis (Renaud and Michaux 2003) and compared the different molars. Based on this data set, we addressed the following questions: (1) are the teeth along a molar row highly integrated, according to the predictions of the developmental and genetic data? (2) Are the teeth of occluding molar rows highly integrated, as expected due to the morpho-functional constraints related to occlusion? (3) Are the patterns of variation similar in the two species, despite the time elapsed since their divergence?

MATERIALS AND METHODS

Material

The house mice (*M. musculus domesticus*) were trapped in Gardouch (43°2N, 01°4E) near Toulouse (South-western France). The

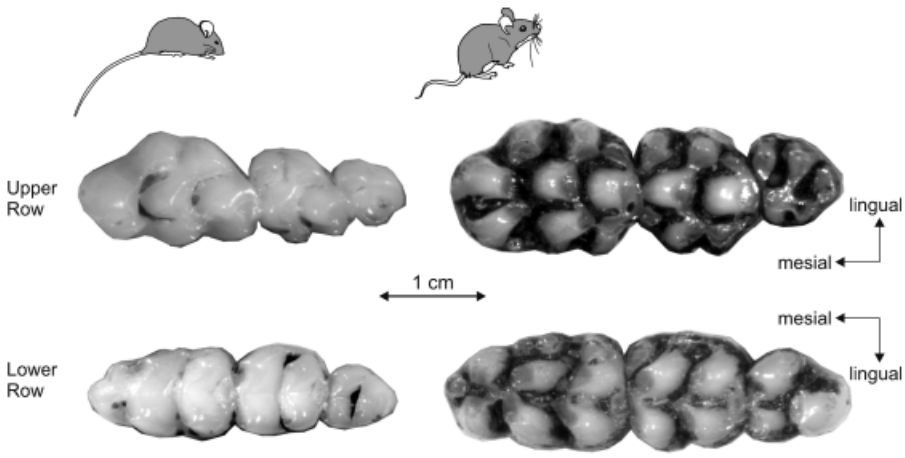

Fig. 1. Example of right upper and lower molar rows of the house mouse (*Mus musculus domesticus*, Gardouch, France), to the left, and of the wood mouse (*Apodemus sylvaticus*, Tourch, France), to the right.

population was flourishing due to food supply in a roe deer farming area. The wood mice (*A. sylvaticus*) were trapped in Tourch (48.0°N, 3.8°W) (Brittany, France). The wood mouse is the only *Apodemus* species present in Brittany (Le Louarn and Quéré 2003), thus avoiding the risk of a mixture with other species difficult to distinguish based on phenotypic criteria, such as the yellow-necked mouse *Apodemus flavicollis*. Subsequently the molars are labelled as follows: UM for upper molars and LM for lower molars, LM2 being the second lower molar. For most animals, the animal length (= head+body) was available, providing an estimate of body size.

Animals with all the six molars intact have been included in the analysis, namely 64 house mice and 88 wood mice. Only specimens with erupted third molars were considered, because corresponding to adult and sub-adult animals after weaning. Old animals displaying deeply worn teeth were scarce; they were anyway discarded because usually at least one of the molars was broken and could not be measured.

To assess a possible impact of wear on molar variation, animals were classified according to their tooth wear stage (WS), evaluated on the upper molar row (modified after Adamczewska-Andrzejewska 1967; Steiner 1967; Renaud 2005). The first class (WS1) included specimens with an erupted third molar without traces of wear. Because WS1 animals were very seldom found, they were pooled with WS2 animals displaying slightly worn cusps. WS3 included specimens with surfaces of all cusps tending to join on the third upper molar, and forming a ring of cusps on UM2 and UM1. WS4 corresponded to individuals with a much worn chewing surface, the enamel loops circumscribing the base of the cusps. The last class WS5 was characterized by all molars worn flat, only the UM1 possibly showing some rest of cusps. The frequency of these classes provided hints about the age structure in the population. The house mouse population from Gardouch was of balanced composition with most of the animals corresponding to WS3 (WS1–2: 30%; WS3: 57%; WS4: 10%; WS5: 2%). The wood mouse population from Tourch corresponded to a younger population (WS1–2: 51%; WS3: 47%; WS4: 2%; WS5: 0%). This is in agreement with season of trapping (autumn for the wood mice of Tourch, the population being thus dominantly composed of young animals born in summer; spring for the house mice of Gardouch, hence including older, overwintered animals).

Outline analysis

The outline of the tooth registers the differences in relative position and importance of the main cusps. Hence, it is appropriate to describe the overall morphology of the molars in murine rodents, as exemplified by studies of first upper and lower molars evolution along fossil lineages (e.g., Renaud et al. 1996; Renaud and van Dam 2002), and of geographic variation within the wood mouse (Renaud and Michaux 2007) and the house mouse (Cucchi et al. 2006; Michaux et al. 2007).

The outline considered here corresponds to the two-dimensional (2D) projection of the tooth viewed from the occlusal surface, with focus at the base of the crown. The 2D projection presents the advantage to be relatively invariant with the degree of wear of the molars (Renaud 2005).

For each tooth, 64 points at equally spaced intervals along the outline were sampled. Two main Fourier methods can be applied to this data set. Firstly, a radial Fourier transform (RFT) calculates the distance of each point to the center of gravity of the outline (e.g., the radius). A Fourier transform is then applied to these 64 radii values (Renaud and Michaux 2003), describing the original data as a sum of trigonometric functions of decreasing wavelength, the harmonics. The outline is accordingly described by a set of Fourier coefficients (FCs) A_n and B_n weighting each harmonic. The zero harmonic amplitude is proportional to the size of the outline and is used to standardize all FCs in order to retain shape information only.

The second method corresponds to the elliptic Fourier transform (EFT). This method is based on separate Fourier decompositions of the incremental changes along x and y as a function of the cumulative length along the outline (Kuhl and Giardina 1982). Any harmonic corresponds to four coefficients: A_n and B_n for x, and C_n and D_n for y, defining an ellipse in the xy plane. The coefficients of the first harmonic, describing the best-fitting ellipse to the original outline, are used to standardize the size, orientation, and starting point of the object. These standardizations constitute a major advantage of the EFT; yet, the FCs are somehow redundant because the variations along x and y are related when considering a closed outline.

Because the present study aimed to analyze patterns of (co-) variation, it is preferable to minimize the measurement error and the number of variables. Hence, a combination of both methods ("REFT") was used to optimize on the one hand, the standardization of the outlines according to orientation and starting point, and on the other hand, a minimal number of variables. EFT was applied to the 64 points of the outline, and a reconstructed outline of each tooth was obtained, the orientation being standardized according to the major axis of the first ellipse, and the starting point as the intersection of the outline with this major axis. The reconstructed outline was described by 64 points as the original, without loosing much detail in the outline because 16 harmonics were retained (i.e., 64 FCs for 64 initial points). RFT was then applied to the new 64 points, obtaining a set of FCs standardized by size.

This combined procedure was applied to the analysis of the three upper molars and the first lower molars. For these teeth, the starting point was difficult to determine with confidence as it would correspond to maximum degree of curvature, whereas the pronounced elongation of their shape provided a reproducible orientation of the first ellipse. The second and third lower molars were analyzed using the direct RFT procedure, because a starting point could be reliably defined at the intersection of the outline with the central gutter delimited by the two rows of cusps, whereas the direction of the first ellipse might have been unstable, because of their stocky shape.

A characteristic of the Fourier analysis is that the higher the rank of the harmonic, the more details of the outline it describes. Hence, for simple shape, like murine molars, the contribution of the harmonic decreases as their rank increases whereas the amount of measurement error increases concomitantly (e.g., Renaud and Michaux 2003). To estimate the rank of the last harmonic to be considered in the subsequent analyses, measurement error was estimated on a randomly chosen house mouse and wood mouse, for which the six molars have been repeatedly measured 15 times on three different days, skull and mandible being repositioned each time with readjustment of lighting.

Size and shape descriptors

The length of the whole upper (UMR) and lower (LMR) molar row was measured. Molar size was estimated for each molar as the 2D-outline area. The square root was considered in order to eliminate quadratic effects. The shape of each molar was described by a set of FCs.

The amount of size variance was estimated as the variance and/or the coefficient of variation of the square-rooted area. The shape variance was estimated as the trace (i.e., the sum of the diagonal elements) of the variance co-variance (VCV) matrix of the FCs. Each data set was bootstrapped 100 times, and the size and shape variance were estimated for these bootstrapped samples. Their variability provided an estimate of the robustness of the variance estimates regarding sampling.

Size and shape co-variation

The size variations of the different molars were compared using linear regression, the most anterior molar along the molar row being the independent size variable. Upper molar size was considered the independent variable when compared with lower molar size.

Co-variation in shape between the different molars was estimated in several ways, in order to investigate the performance of different approaches and obtain a cross-validation of the most reproducible results. Two fully multivariate comparisons were applied. First, co-variation among molars was analyzed using a multivariate multiple regression in which several dependent variable (here the FCs of a molar) are regressed simultaneously onto more than one independent variables (here the FCs of another molar) (Rohlf 2007). Procedures for comparison were similar to those for size comparisons. The test considered was the Wilks Lambda test. In complement, matrices of distance among individuals were computed for each molar, based on Euclidean distance among FCs. These distance matrices were compared using a Mantel *t*-test, providing an *R* value, and a probability that the observed correlation was higher than random, based on 1000 permutations.

Finally, to evaluate if co-variation among molars corresponded to major directions of phenotypic variance, the direction of greatest variance was calculated for the six molars and the two populations as the first eigenvector (V1) of the VCV matrix of the FCs. Scores of the specimens along the V1 vectors were compared among molars to check for a co-variation. Statistics were performed using NTSYSpc 2.2 (Rohlf 2007) and SYSTAT 12.

Comparison of main directions of variation and co-variations

Significant shape changes involved in the co-variation were visualized using Partial Least Squares (PLS) analysis (Rohlf and Corti 2000). This multivariate technique decomposes the matrix of the co-variance between two sets of variables, here the sets of FCs of two different molars into principal axes, one for each set of variables. Reconstructed outlines corresponding to these vectors can visualize the shape changes involved in the co-variation of two molars.

These vectors of co-variation were estimated for the house mouse and the wood mouse populations. To evaluate if the patterns of co-variation were conserved among the two species, the first vectors obtained for any PLS analysis were compared between the two species. Finally, the shape change due to co-variation among molars (PLS vectors) was compared with the main directions of variation within the populations (V1 vectors).

The correlations among these vectors were estimated knowing that the angle between two vectors is the arc cosine of the inner product of the two vector elements. Simulation of angles between random vectors was used to assess the statistical significance of this correlation (Klingenberg 1996; Renaud et al. 2006). Fifty thousand simulations were performed. They provided the following significance threshold for the absolute value of the inner product "*R*": probability that the observed *R* is higher than random: $P>0.95$, $R=0.681$; $P>0.99$, $R=0.814$; $P>0.999$, $R=0.904$.

RESULTS

Measurement error and selection of relevant shape descriptors

The amount of information brought by the successive harmonics approximating the initial outline is proportional to the harmonic amplitude (i.e., the square root of the squared FCs). For both the house and the wood mouse (Fig. 2, A and C), the amplitude was relatively high until the fourth harmonic, decreased to a low plateau until the eighth, being subsequently close to zero. Concomitantly measurement error (coefficient of variation of the harmonic amplitude among the repeated measurements) increased from the fourth harmonic onwards (Fig. 2, B and D). Hence, the fourth harmonic was chosen as a threshold offering a satisfying compromise between measurement error and information content for the six molars of the two species.

Size and shape variance

Size and shape variances were evaluated for the six molars and compared. To correct for absolute differences in tooth size, the coefficient of variation was considered for size. Shape variance was estimated by the sum of the variance of the eight retained FCs.

Size variance (Fig. 3, A and C) increased from the first to the third molars, the pattern being more equilibrated in the wood mouse than in the house mouse. Shape variance in the two species (Fig. 3, B and D) displayed similar pattern of increased variance along the tooth row, especially due to the high variance of the UM3 and LM3.

The amount of error tended to increase from the first to the lower molar. However, the corresponding variance remained low compared with the variance within sample, suggesting that the observed increasing variance of the third molars may reflect actual differences and not only artifact due to measurement error. The only exception is the wood mouse LM3 that displayed a dramatic amount of error. This might be characteristics of the randomly chosen specimen, because it has been observed by the operator (S. R.) that the outline of some third molars is sometimes difficult to make out, due to sloping back-part of the tooth. The high mea-

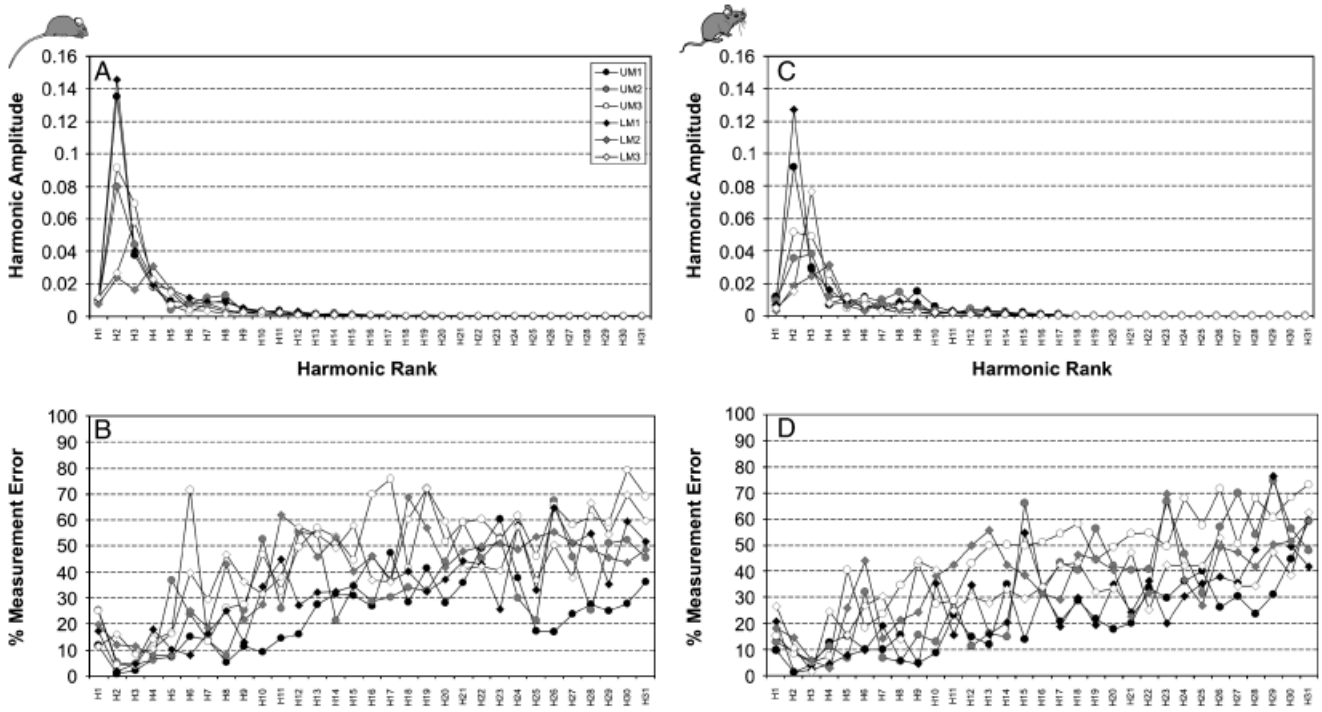

Fig. 2. Harmonic amplitude and measurement error as a function of harmonic rank for a house mouse (A and B) and a wood mouse (C and D), for the three upper and three lower molars. Harmonic amplitude (A and C) is the square-root of the sum of the Fourier coefficients. Measurement error (B and D) is estimated as the coefficient of variation of the harmonic amplitude, based on 15 repeated measurement of a randomly chosen specimen.

surement error may thus be a corollary of the high morphological variance of this tooth.

Size co-variation

Most of the regressions between molar sizes were highly significant for the house mouse (Table 1) and the wood mouse (Table 2). The strongest relationships (Fig. 4, A and C) related not only molars within but also across molar rows, especially between occluding molars at the same position along the molar row (e.g., UM1–LM1). Relationships involving the third molars were overall weaker in wood mice than in house mice. Wear affected only slightly molar size for the house mouse (UM3: $P = 0.049$; LM1: $P = 0.002$; nonsignificant for other molars) and no significant effect was detected for the wood mouse. Accordingly, patterns emerging when considering relationships within the dominant WS only (WS3 for the house mouse, WS2 within the wood mouse) were similar to those observed for the whole population.

Strong size co-variations among all teeth may be the mere result of a co-variation with overall molar size that was estimated by the length of the molar rows. Upper and lower molar row length are of course correlated (house mouse: $R^2 = 0.640$, $P < 0.001$; wood mouse: $R^2 = 0.541$, $P < 0.001$). Molar size was regressed onto molar row length, and the residuals were compared among teeth. Significant relationships persisted in the house mouse population; patterns were, however, more complex because the relationship was positive for UM1–LM1, UM2–LM2, UM3–LM3, LM1–LM2, but also negative for UM1–UM3 and LM1–LM3. A similar pattern emerged for the wood mouse, with positive relationships between UM1 and LM1, UM2 and UM3, UM2 and LM2, UM3 and LM3, LM1 and LM2, and negative between UM1 and UM3.

In contrast to among-molar relationships, molar and body size were weakly correlated (Tables 1 and 2), the LM1 size for the house mouse and the UM3 size for the wood mouse being the only one significantly correlated with body size.

Shape co-variation

Relationships among molar shape were not as strong as for molar size, possibly because it is more difficult to evidence significant co-variation on a multivariate data set. Yet, numerous multivariate regressions were significant (Tables 3 and 4; Fig. 4, B and D), relating teeth within a molar row but also across molar rows. They were not limited to occluding teeth in the same position along the molar row but evidenced a broader integration among the molar rows (e.g., UM2–LM1, UM1 and LM2). Co-variations involving third molars were particularly week and it was the only position where no correlation between occluding teeth was detected in the house mouse.

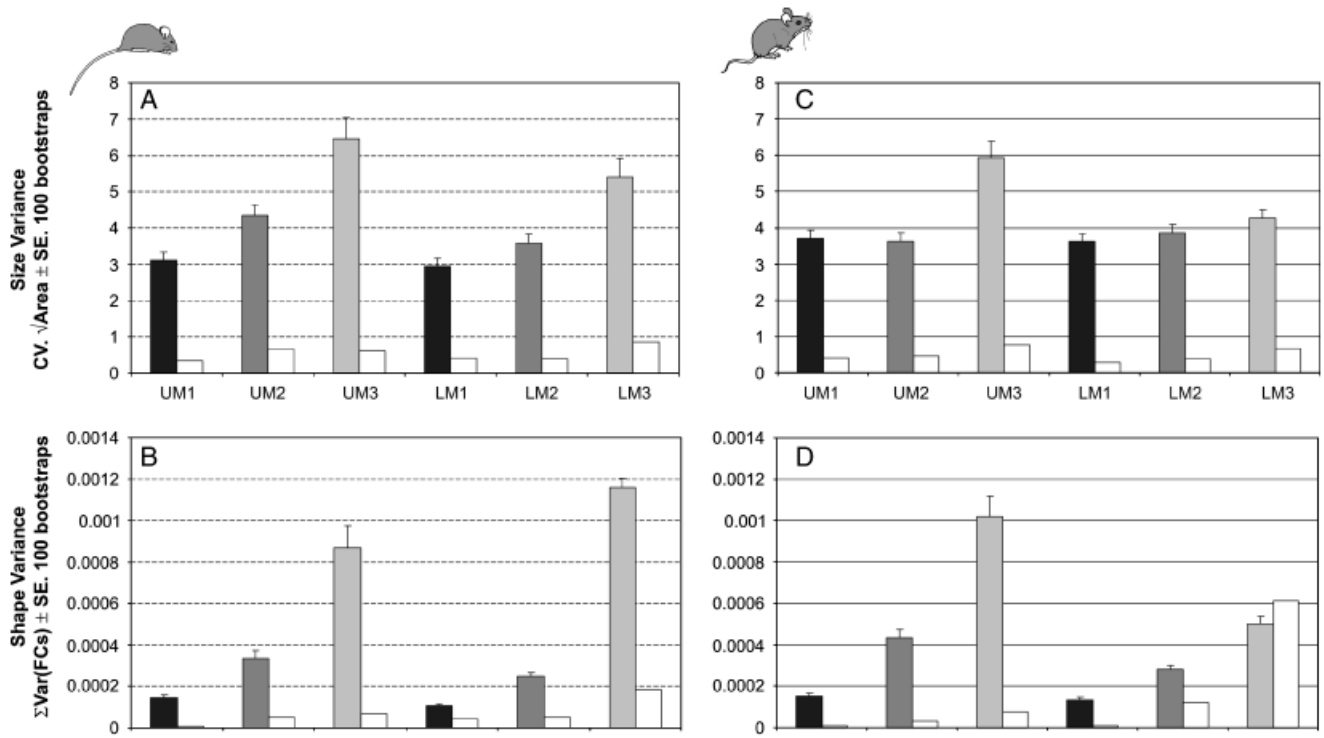

Fig. 3. Size and shape variance of the six molars for the house mouse (A and B) and the wood mouse (C and D). Size (A and C) was estimated by the square-root of the area of the 2D molar outline; its variance was estimated by the coefficient of variation. Shape variance (B and D) was estimated as the trace (sum of the diagonal elements) of the variance co-variance (VCV) matrix of the Fourier coefficients. For size and shape, error bars correspond to the standard error of the variance estimates in 100 bootstraps of the initial samples, and variance due to measurement error for each tooth is indicated as open bar close to the variance of each sample.

Along the adult life of the animal, body size slightly increases and teeth are progressively worn. Wear might cause apparent co-variation in molar shape that would not be due to common genetic background or developmental interactions. A significant effect of WS was found on molar shape in the house mouse population (UM1, UM2, LM2: $P<0.001$; LM3: $P=0.002$; LM1: $P=0.011$; UM3: $P=0.053$), a much weaker effect being evidenced in the younger wood mouse population (UM1: $P=0.011$, all other tests not significant). The possible effect of wear on co-variation pattern was tested by restricting the comparisons among molars to the dominant WS within the population. This diminished the sample size (38 for WS3 of the house mice, 45 for WS2 of the wood mice). Trends were similar to those obtained on the whole population, but fewer probabilities were significant due to the poorer sampling. Significant relationships persisted between

Table 1. Linear regression between the size of the different molar teeth in the house mouse population (*Mus musculus domesticus*) of Gardouch

	√ArUM1	√ArUM2	√ArUM3	√ArLM1	√ArLM2	√ArLM3	Body
√ArUM1	—	**0.000**	**0.000**	**0.000**	**0.000**	**0.000**	0.198
√ArUM2	0.495	—	**0.000**	**0.000**	**0.000**	**0.000**	0.774
√ArUM3	0.248	0.650	—	*0.024*	**0.000**	**0.000**	0.335
√ArLM1	0.531	0.163	0.078	—	**0.000**	*0.026*	**0.002**
√ArLM2	0.554	0.506	0.250	0.728	—	**0.000**	0.239
√ArLM3	0.238	0.567	0.624	0.075	0.343	—	0.410
Body	0.025	0.001	0.014	0.138	0.022	0.011	—

Below the diagonal, R^2 values; above the diagonal P value of the regression. In italics, $P<0.05\%$; after a Bonferroni correction, significance threshold is $P_{05\%}=0.05/21=0.002$ (in bold).
Body size of the animals is estimated by the animal length, that is head+body length. Upper molars (UM) and lower molars (LM) size is estimated by the square root of their area.

Table 2. Linear regression between the size of the different molar teeth in the wood mouse population (*Apodemus sylvaticus*) of Tourch

	√ArUM1	√ArUM2	√ArUM3	√ArLM1	√ArLM2	√ArLM3	Body
√ArUM1	—	**0.000**	**0.007**	**0.000**	**0.000**	**0.000**	0.589
√ArUM2	0.508	—	**0.000**	**0.000**	**0.000**	**0.000**	0.853
√ArUM3	0.081	0.397	—	*0.012*	**0.000**	**0.000**	*0.024*
√ArLM1	0.747	0.457	0.072	—	**0.000**	**0.000**	0.654
√ArLM2	0.579	0.647	0.184	0.719	—	**0.000**	0.327
√ArLM3	0.157	0.313	0.408	0.168	0.315	—	0.138
Body	0.003	0.000	0.058	0.002	0.011	0.025	—

Below the diagonal, R^2 values; above the diagonal P value of the regression. In italics, $P<0.05\%$; after a Bonferroni correction, significance threshold is $P_{05\%} = 0.05/21 = 0.002$ (in bold).
Body size of the animals is estimated by the head+body length. Upper molars (UM) and lower molars (LM) size is estimated by the square root of their area.

UM1 and UM2, UM1 and LM1, UM2 and LM2, and LM1 and LM2 for the house mouse, and UM1 and UM2, UM1 and LM2, LM1 and LM2 for the wood mouse.

Molar shape was further compared with body size, estimated by animal length, using a multivariate regression. No significant relationship of molar shape with body size was evidenced, except for UM1 and UM2 in house mice (Table 3), and LM1 in wood mice (Table 4). These results showed that the co-variations among molars were not due only to an artifact related to WS or animal size.

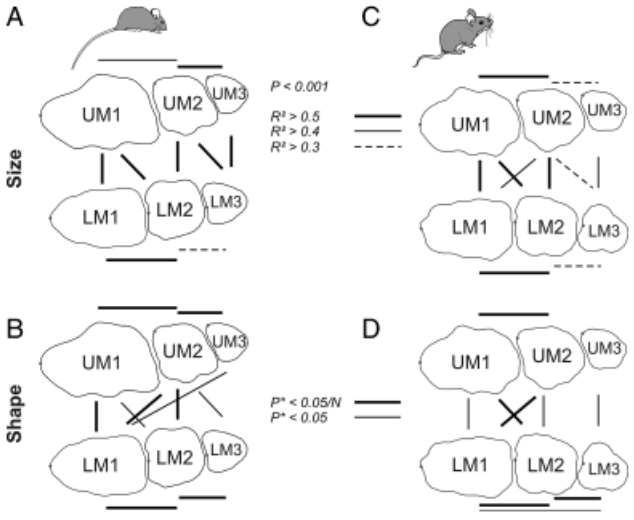

Fig. 4. Patterns of size and shape co-variation among molars for the house mouse (A and B) and the wood mouse (C and D). Significant probabilities are indicated by lines relating the corresponding molars. For size (A and C), almost all probabilities based on linear regressions were highly significant. Differences in the strength of the relationship were indicated based on the coefficient of correlation R^2. Thick lines $R^2>0.5$; medium lines $R^2>0.4$; dotted line $R^2>0.3$. The graph for shape co-variation (B and D) illustrates results of the multivariate regression between the FCs. Thick lines: $P<0.05\%$ with a Bonferroni correction; medium line $P<0.05\%$.

The approach based on multivariate regressions was complemented by a comparison of distance matrices (Tables 5 and 6). The pattern was overall the same, with high correlations within a molar row (especially M1–M2) but also among molar rows, e.g., UM1–LM2 in both species and UM2–LM1 in wood mice.

Finally, correlations among main directions of intragroup variance, estimated as the first eigenvector (V1) of the VCV matrix of the different molars were investigated. The V1 vector represented between 30% and 54% of the total variance in house mice (Table 7) and 37–61% in wood mice (Table 8). The pattern of correlations was similar to the one provided by the other method. Correlations were overall higher in wood mice than in house mice, possibly because of the higher number of specimens (88 instead of 64) allowing a better estimate of the eigenvectors.

The congruent patterns of co-variation between the different analyses can be summarized by the following relationships being the most stable whatever the method and the species: UM1–UM2, UM1–LM1, UM1–LM2, UM2–LM2, and to a lesser degree LM1–LM2 and LM2–LM3.

Comparison of main directions of variation and co-variation

PLS analyses among teeth of the house mouse (Fig. 5(1)) have been performed to visualize the co-variation between UM1, UM2, LM1, and LM2. We focused on the first direction of co-variation that explained a high percentage of the total co-variation ($>50\%$ in all the cases and $>85\%$ when involving UM1) (Table 9). In all cases considered, the molars of a same animal shared either a slender, angular outline, or rounded and broad shape (Fig. 5(1)). The broadening of the tooth did not involve a relative shifting of the cusps, but the cusps were transversally more massive. According to this pattern a slender UM1 was associated with an elongated and triangular UM2, and slender UM1 were associated with slender LM1 (Fig.

Table 3. Multiple regression between molar shape descriptors in the house mouse population (*Mus musculus domesticus*) of Gardouch, and between shape descriptors and animal length, used as proxy for body size

	$UM1_{REFT4}$	$UM2_{REFT4}$	$UM3_{REFT4}$	$LM1_{REFT4}$	$LM2_{RFT4}$	$LM3_{RFT4}$
$UM1_{REFT4}$	—					
$UM2_{REFT4}$	**0.0000**	—				
$UM3_{REFT4}$	0.5352	**0.0018**	—			
$LM1_{REFT4}$	**0.0011**	**0.0007**	*0.0039*	—		
$LM2_{RFT4}$	*0.0075*	**0.0002**	0.7405	**0.0000**	—	
$LM3_{RFT4}$	0.3488	0.0127	0.3516	0.2176	**0.0026**	—
Body length	**0.0023**	**0.0000**	0.2591	0.1520	0.3498	0.8198

Shape of each character is described by the Fourier coefficients of its outlines. Probability of the Wilks Lambda test is given. In italics, $P<0.05\%$; after a Bonferroni correction, significance threshold is $P_{05\%} = 0.05/15 = 0.0033$ (in bold).

5(1)B), whereas among second molars, angular second molars (triangular for UM2, squared for LM2) were opposed to rather roundish UM2–LM2 pairs (Fig. 5(1)C). Other changes seemed to involve more localized morphological changes. It was especially the case of the co-variation within the lower molar row (Fig. 5(1)D). The broadening versus slenderizing of the LM1 seemed localized at the back-part of the tooth, whereas the associated LM2 were rounded versus squared.

Results were rather similar considering the wood mouse (Fig. 5(2)). The first direction of co-variance extracted by the PLS analysis represents an even higher percentage of the total co-variance (>75% and up to 93%; Fig. 5(2)). In most of the cases, the major patterns of co-variation corresponded to changes in overall tooth shape: elongated versus broad teeth, angular versus roundish teeth. This was the case within the upper molar row (Fig. 5(2)A), elongated UM1 being associated with rather triangular UM2, opposed to broad UM1-squared UM2. Within the upper molar row (Fig. 5(2)A), elongated UM1 were associated with rather triangular UM2, opposed to broad UM1-squared UM2. Within the lower molar row (Fig. 5(2)D), elongated LM1 were associated with rectangular LM2 and opposed to short, massive LM1 and LM2. Across molar rows (Fig. 5(2), B and C), slender first molars were opposed to first molars characterized by a broadening of their back-part, as for the house mouse. This may correspond to a more or less developed lingual margin on the LM1 (Fig. 1). Triangular UM2 were associated with rectangular LM2, being opposed to the pair squared, massive UM2/squared massive LM2.

Comparing the directions of co-variations observed for the house mouse and the wood mouse (Table 9) evidenced that patterns of co-variation were overall conserved among both species, especially regarding the first molars: UM1 in the UM1–UM2 comparison, LM1 in the LM1–LM2 comparison, and both UM1 and LM1 in the UM1–LM1 comparison (Table 9). Among these correlated directions, the most conserved among species are those regarding the co-variation between UM1 and LM1, opposing in both cases slender to broader molars.

Finally, the major directions of co-variations extracted by the PLS analyses were compared with the major directions of variation for each tooth (Table 10). In most of the cases, and especially for the wood mouse, these major directions of variation per character, and co-variation among characters, were highly correlated (Table 10). This means that the teeth mostly changed in a concerted way.

Table 4. Multiple regression between molar shape descriptors in the wood mouse population (*Apodemus sylvaticus*) of Tourch, and between shape descriptors and animal length, used as proxy for body size

	$UM1_{REFT4}$	$UM2_{REFT4}$	$UM3_{REFT4}$	$LM1_{REFT4}$	$LM2_{RFT4}$	$LM3_{RFT4}$
$UM1_{REFT4}$	—					
$UM2_{REFT4}$	**0.0000**	—				
$UM3_{REFT4}$	0.2604	0.7772	—			
$LM1_{REFT4}$	*0.0087*	**0.0013**	0.9989	—		
$LM2_{RFT4}$	**0.0001**	*0.0114*	0.6309	**0.0000**	—	
$LM3_{RFT4}$	0.0815	0.0747	*0.0440*	*0.0038*	**0.0006**	—
Body length	0.4949	0.6351	0.5686	*0.0197*	0.0929	0.2235

Shape of each character is described by the Fourier coefficients of its outlines. Probability of the Wilks Lambda test is given. In italics, $P<0.05\%$; after a Bonferroni correction, significance threshold is $P_{05\%} = 0.05/15 = 0.0033$ (in bold).

Table 5. Correlations between molar shape distances within the house mouse population (*Mus musculus domesticus*) of Gardouch

	$UM1_{REFT4}$	$UM2_{REFT4}$	$UM3_{REFT4}$	$LM1_{REFT4}$	$LM2_{RFT4}$	$LM3_{RFT4}$
$UM1_{REFT4}$	—	**0.0020**	0.9650	*0.0310*	*0.0170*	0.4046
$UM2_{REFT4}$	0.235	—	*0.0120*	0.1738	*0.0250*	0.5255
$UM3_{REFT4}$	− 0.123	0.182	—	*0.0410*	0.3746	0.1409
$LM1_{REFT4}$	0.142	0.066	0.134	—	*0.0260*	0.5574
$LM2_{RFT4}$	0.134	0.126	0.021	0.131	—	0.1089
$LM3_{RFT4}$	0.008	0.009	0.079	− 0.010	0.074	—

Euclidean distances were calculated among the 64 specimens based on the Fourier coefficients (REFT/RFT4) of their outline. Distance matrices were compared by Mantel tests. Below the diagonal, *R* values; above the diagonal probability that the observed correlation is higher than among random samples (1000 permutations). In italics, $P<0.05\%$; after a Bonferroni correction, significance threshold is $P_{05\%} = 0.05/15 = 0.0033$ (in bold).

DISCUSSION

A strong integration in both size and shape between murine molars

Our results first evidenced a strong integration within and among molar rows. Such a strong integration, based on patterns of correlations among size-related measurements, has already been shown in diverse species, especially carnivores (e.g., Kurtén 1967; Szuma 2000; Prevosti and Lamas 2006). The fact that the size of all teeth in an apparatus vary in the same way has been suggested to be the result of a common relationship to the body size of the animal (Kurtén 1967). This explanation, however, is undermined in our case by the very weak or inexistent relationship found among tooth size and body size of the mice. Strong integration among molar sizes may alternatively be the indirect result of a high integration between molar rows as a whole. Indeed, controlling molar row length lessens by a significant degree the number of significant interactions among molar sizes. Yet, several significant relationships persisted that exemplify complex balances in tooth sizes along the molar row.

To such data based on tooth size, the originality of the present study is to add data on molar shape, a much more complex character to analyze. Overall the level of integration appears weaker regarding shape than size. This effect may be an artifact of multivariate comparisons, for which it may be more difficult to reach significance threshold than for univariate correlations. This may also be a consequence of the shape complexity compared with tooth size: differences in tooth shape involve relative breadth but also spatial shifts of cusps and their relative development in relation with each other. Hence, relationship among tooth shape might involve much finer mechanisms controlling the precise position and size of the cusps.

Co-variation within molar row: the signature of developmental integration?

Despite the apparent lesser integration in shape than in size, emerging patterns of co-variation are remarkably similar based on molar size and shape (Fig. 4). Co-variations between adjacent and occluding teeth are particularly marked, a pattern already reported in other mammals (Kurtén 1967; Szuma 2000; Prevosti and Lamas 2006).

The high integration between adjacent teeth within a molar row was expected based first on the "neighboring rule," that is, spatial interactions due to contiguity during development

Table 6. Correlations between molar shape distances within the wood mouse population (*Apodemus sylvaticus*) of Tourch

	$UM1_{REFT4}$	$UM2_{REFT4}$	$UM3_{REFT4}$	$LM1_{REFT4}$	$LM2_{RFT4}$	$LM3_{RFT4}$
$UM1_{REFT4}$	—	*0.010*	0.8392	*0.0050*	*0.0120*	0.3257
$UM2_{REFT4}$	0.137	—	0.1159	0.1858	**0.0020**	0.0719
$UM3_{REFT4}$	− 0.054	0.065	—	0.5035	0.1628	0.9191
$LM1_{REFT4}$	0.148	0.043	0.006	—	**0.0010**	0.8492
$LM2_{RFT4}$	0.132	0.186	0.046	0.240	—	0.9011
$LM3_{RFT4}$	0.020	0.075	− 0.064	− 0.046	− 0.064	—

Euclidean distances were calculated among the 64 specimens based on the Fourier coefficients (REFT/RFT4) of their outline. Distance matrices were compared by Mantel tests. Below the diagonal, *R* values; above the diagonal probability that the observed correlation is higher than among random samples (1000 permutations). In italics, $P<0.05\%$; after a Bonferroni correction, significance threshold is $P_{05\%} = 0.05/15 = 0.0033$ (in bold).

Table 7. Linear regressions between major directions of shape variance of the different molars in the house mouse population (*Mus musculus domesticus*) of Gardouch

	%V1	%V2	V1UM1	V1UM2	V1UM3	V1LM1	V1LM2	V1LM3
V1UM1	48.9	24.4	—	**0.001**	0.938	**0.002**	*0.011*	0.389
V1UM2	53.8	17.6	0.179	—	0.142	0.279	*0.005*	0.072
V1UM3	44.3	35.2	0.000	0.034	—	0.063	0.287	0.554
V1LM1	47.8	21.4	0.146	0.019	0.054	—	0.530	0.372
V1LM2	40.5	29.9	0.099	0.121	0.018	0.006	—	*0.033*
V1LM3	30.2	29.9	0.012	0.051	0.006	0.013	0.071	—

Major direction of variance is estimated as scores on first eigenvector (V1) of the variance co-variance matrix of the Fourier coefficients. The two columns left indicate the percentage of variance for the first two eigenvectors V1 and V2. Below the diagonal, R^2 values (percentage of variance explained by the regression); above the diagonal P value of the regression. In italics, $P<0.05\%$; after a Bonferroni correction, significance threshold is $P_{05\%} = 0.05/15 = 0.003$ (in bold).

(Van Valen 1970). It was further expected based on developmental data, because a common set of genes contributes to determine the early molar morphogenetic field that will give rise to the whole molar row (e.g., Tucker and Sharpe 2004). Latern interactions during the development of the row may strengthen the integration among teeth of a molar row, because experimental data have shown an inhibitory effect of the first developing molar on the second, and of the second on the third molar, making the interaction of the first on the third molar an indirect one mediated by the second molar (Kavanagh et al. 2007). Our data indeed strongly support an influence of M1 on M2 and of M2 on M3, regarding both size and shape. It is striking, that molar size corrected by molar row length makes negative relationship emerge between M1 and M3, in full agreement with the cascade model proposed by Kavanagh et al. (2007).

Increased variance from the first to the third molar

This cascade of influences along the molar row leads to the expectation that the latter forming teeth would be the most variable, because any difference in the genotype as well as any perturbation during development of the earlier teeth may accumulate and be magnified at the end of the cascade. Accordingly, we observed that the third molars were the most variable, the second molar being intermediate in variance.

Alternate hypotheses have, however, been advanced to explain differences in variation levels of teeth in various animal models (Gingerich and Schoeninger 1979; Szuma 2000; Dayan et al. 2002). Small teeth may be the most variable because small-sized features would display an increased measurement error (Polly 1998); or small vestigial teeth would be under lower stabilizing selection and hence more variable (Gingerich and Schoeninger 1979).

Indeed the third molar in murine rodents is by far the smallest of the teeth and its measurement error tended to be high. However, variation due to error was small compared with the total variance in most of the cases, suggesting that it could not account for the whole pattern. The third molar is also reduced in murine rodents, even missing in some species (Misonne 1969), or in some specimens, e.g., in *M. musculus* or *Mus pahari*. It is thus of less importance for an efficient oc-

Table 8. Linear regressions between major directions of shape variance of the different molars in the wood mouse population (*Apodemus sylvaticus*) of Tourch

	%V1	%V2	V1UM1	V1UM2	V1UM3	V1LM1	V1LM2	V1LM3
V1UM1	50.5	15.6	—	**0.003**	0.073	**0.000**	**0.001**	0.870
V1UM2	57.5	17.2	0.097	—	0.070	**0.002**	**0.000**	*0.019*
V1UM3	61.4	14.6	0.037	0.038	—	0.576	0.296	0.391
V1LM1	53.1	18.5	0.182	0.103	0.004	—	**0.000**	0.742
V1LM2	37.4	25.7	0.124	0.246	0.013	0.215	—	*0.012*
V1LM3	37.3	31.2	0.000	0.062	0.009	0.001	0.071	—

Major direction of variance is estimated as scores on first eigenvector (V1) of the variance co-variance matrix of the Fourier coefficients. The two columns left indicate the percentage of variance for the first two eigenvectors V1 and V2. Below the diagonal, R^2 values (percentage of variance explained by the regression); above the diagonal P value of the regression. In italics, $P<0.05\%$; after a Bonferroni correction, significance threshold is $P_{05\%} = 0.05/15 = 0.003$ (in bold).

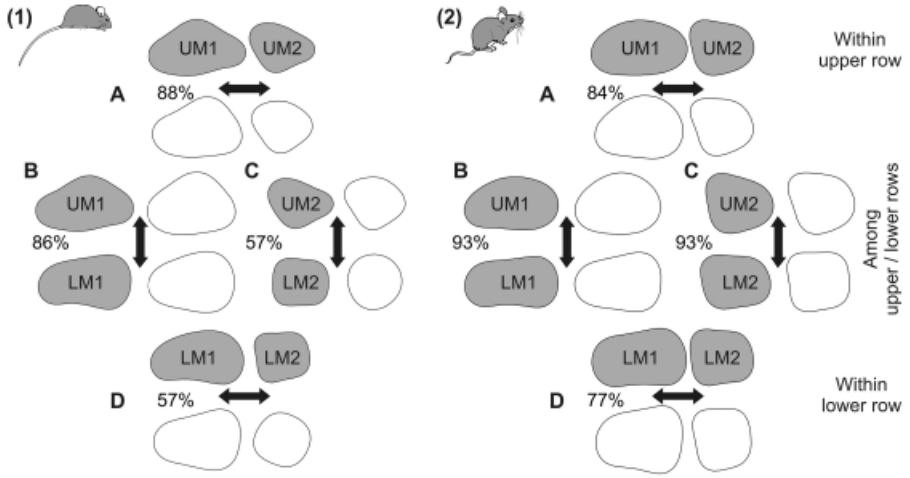

Fig. 5. Shape changes involved in the co-variation, based on Partial Least Squares analyses for the house mouse (1) and the wood mouse (2). Four analyses are presented: (A) co-variation between the first and the second upper molars (UM1–UM2); (B) UM1–LM1; (C) UM2–LM2; (D) LM1–LM2. For each PLS analysis two pairs of outlines are presented, corresponding to PLS first axes = 0.03 (gray outlines)/ – 0.03 (white outlines).

clusion. However, the third molars also appear as most variable in large mammals such as goats where it is as large as other molars (Natsume et al. 2008). This suggests that the reduced functional constraint is not the only factor contributing to the increased variance.

All these hypotheses are not mutually exclusive and may contribute to the observed pattern of the third molar as the most variable. The magnified variance from the first to the third molar may further explain that the strength of co-variation decreases along the molar rows and that few significant relationship among molars involve the third one.

Strong integration between occluding molar rows: an ultimate consequence of functional constraints?

Strong functional interactions relate directly occluding teeth among molar rows. As such, a high genetic integration between them is expected to have evolved in response to the functional demand (Olson and Miller 1958; Cheverud 1982). On the other hand, developmental and genetic data provided less support to an expectation of high integration among occluding molar rows than within molar rows. The requirement of common genes occasionally differ between the upper and lower molar rows (Wang et al. 2005; Charles et al. 2009), and a QTL analysis further evidenced a relative independence between them (Shimizu et al. 2004). Despite this, our results fully support that evolution lead to a high phenotypic integration of functionally related traits (Cheverud 1982), further suggesting that the same genetic networks are responsible for population-level variation in both upper and lower teeth.

These results are in agreement with previous studies based on phenotypic correlations, which evidenced correlations among occluding teeth as a common feature, especially in carnivores (Kurtén 1967; Szuma 2000; Prevosti and Lamas 2006). Concerted variations between occluding teeth are a prerequisite for an efficient occlusion, and hence for the survival of the animal. During mastication in murine rodents, the jaw effects a reduced propalinal movement from the distal bottom to the anterior top (Lazzari et al. 2008b). The LM1

Table 9. Partial Least Squares (PLS) analyses between molar teeth in the house mouse (*Mus musculus domesticus*) and wood mouse (*Apodemus sylvaticus*) populations, and comparison of the directions of co-variation between the two species

	House mouse		Wood mouse		House/wood mouse	
	%V1	%V2	%V1	%V2	Left	Right
UM1–UM2	87.7	7.3	83.6	10.2	0.781	0.640
LM1–LM2	56.6	41.9	76.7	12.9	*0.857*	0.041
UM1–LM1	86.2	10.0	93.1	4.2	**0.947**	**0.932**
UM2–LM2	56.6	39.6	92.5	5.8	– 0.654	-0.647

First two columns: percentage of co-variation represented by the first two PLS vectors for the house mouse; next two columns: idem for the wood mouse; two columns to the right: correlations among the equivalent PLS vectors extracted for the house mouse and the wood mouse populations. "Left" corresponds to the left term in the PLS analysis (UM1 in the UM1–UM2 comparison) and "right" to the right term (UM2 in the UM1–UM2 comparison). In bold $P > 0.999$, $R > 0.904$, in italics $P > 0.99$, $R > 0.814$, underlined $P > 0.95$, $R > 0.681$.

Table 10. Correlations (inner product between vectors) between major directions of co-variation (estimated by a Partial Least Squares [PLS] analysis between two molar teeth), and the major direction of variation V1 of the same two teeth

PLS	V1	HM	WM
UM1–UM2	UM1	*0.824*	**0.917**
UM1–**UM2**	UM2	**0.953**	**−0.981**
LM1–LM2	LM1	*0.844*	**0.960**
LM1–**LM2**	LM2	−0.055	**−0.914**
UM1–LM1	UM1	**−0.987**	**0.986**
UM1–**LM1**	LM1	**0.924**	**0.974**
UM2–LM2	UM2	*0.880*	**0.997**
UM2–**LM2**	LM2	0.480	*−0.886*

HM, house mouse; WM, wood mouse. In bold $P > 0.999$, $R = 0.904$, in italics $P > 0.99$, $R = 0.814$.

starts its movement almost at the posterior border of the UM1 (Fig. 6A), ending with the UM1 anterior-most cusp surrounded by the four anterior cusps of the LM1 (Fig. 6B). Most of the interaction thus occurs between directly occluding teeth and accordingly, the observed pattern of integration reflects functional constraints.

However, co-variation among upper and lower rows also involved molars adjacent to the directly occluding ones, e.g., UM2–LM1 (Fig. 4). Functional contact of such teeth during occlusion is much reduced in murine rodents and their co-variation might rather reflect the integration of the occluding molar rows as a whole. Selection favoring integration among the occluding first molars would easily lead to integration among the other teeth because of the developmental integration within molar row (Kavanagh et al. 2007 and the present results).

Conserved direction of shape variation and co-variation: lines of least resistance to evolution

Our results point to a main direction of molar morphological variation, emerging as directions of major phenotypic variance for each tooth and as major direction of co-variation between teeth. This pattern is conserved between the house mouse and the wood mouse over >10 Ma (Lecompte et al. 2008). Furthermore, the major direction of shape variance of the UM1, opposing slender to broad molars, is comparable to the one found along fossil lineages of murine rodents over >10 Myrs (Renaud et al. 2006). It thus emerges as a general feature in this group of rodents. Such conserved patterns of within-population variation have been advanced to be "lines of least resistance" to evolution by offering a large intrapopulation variance to the screening by selective processes (Schluter 1996). It may be the key to the trend in broadening of the first upper molars as a feature that evolved repeatedly in murine rodents (Renaud and Michaux 2004).

The existence of a major direction of phenotypic variance, corresponding to slender-broader molars, points to a lesser canalization of molars regarding this kind of morphological variation. Possibly, such changes in molar shape have few detrimental consequences for an efficient occlusion, because the longitudinal alignment of the cusps is not modified, as long as upper and lower teeth co-vary in that respect. It is indeed supported by our results that point to a co-variation of the occluding molars according to this pattern of slender versus broader molars. Among the numerous genes involved in molar development, possible candidates for such phenotypic effects are the genes of the EDA pathway. In vivo surexpression of the *Eda* gene during development leads to shorter and wider molars than in control (Mustonen et al. 2003; Kangas et al. 2004). In vitro experimental evidences further suggest that increasing concentration of EDA differentially affect length and width of the primary enamel knot (Penttilä and Jernvall 2008). The existence of intrapopulation differences in EDA expression may thus lead to a variation in relative width of the primary enamel knot that may in turn be translated in variations in the shape of the final teeth, because the dynamics of the enamel knot has been related to differences in final tooth shape (Kangas et al. 2004).

These results point to a high integration between teeth of murine rodents, in agreement with an overall concerted evolution between upper and lower cheek teeth (Misonne 1969). Yet, decoupling between the upper and lower molars has been evidenced in the fossil record (Renaud and van Dam

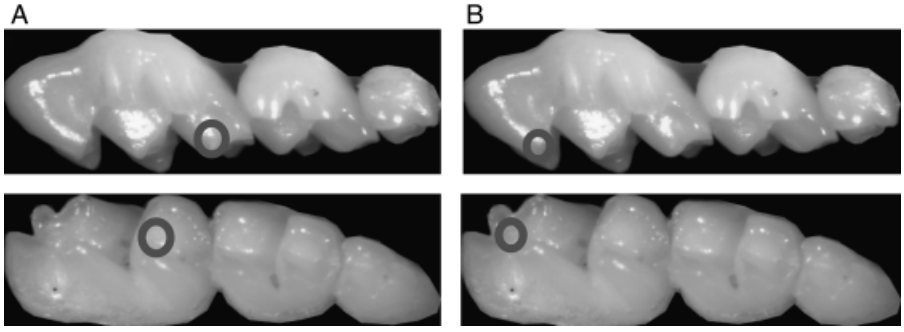

Fig. 6. Occlusion between the upper and lower molar rows, depicted on a specimen of house mouse from Gardouch. Circles represent crucial zones in contact between the first occluding molars. (A) Beginning of the occlusion; (B) end of the occlusion.

2002). Indeed some mutations have a differential impact on the upper and lower molars (e.g., Wang et al. 2005) suggesting that despite a strong and conserved integration with other teeth, decoupling might occur. How such mosaic evolution may occur despite robust integration during evolution is an ongoing challenge for evo-devo studies.

Acknowledgments

We thank Jacques Michaux and Pascale Chevret for stimulating discussions, and we acknowledge the very constructive remarks of both anonymous reviewers. This study has been supported by the ANR "Quenottes" and the GDR 2474 CNRS "Morphométrie et Evolution des Formes." This is the publication ISEM 2009-058.

REFERENCES

Adamczewska-Andrzejewska, K. A. 1967. Age reference model for *Apodemus flavicollis* (Melchior, 1834). *Ekol. Pol., Ser. A* XV: 787–790.

Charles, C., Pantalacci, S., Peterkova, R., Tafforeau, P., Laudet, V., and Viriot, L. 2009. Effect of *Eda* loss of function on upper jugal tooth morphology. *Anat. Rec.* 292: 299–308.

Cheverud, J. M. 1982. Phenotypic, genetic, and environmental morphological integration in the cranium. *Evolution* 36: 499–516.

Cucchi, T., et al. 2006. A new endemic species of the subgenus *Mus* (Rodentia, Mammalia) on the Island of Cyprus. *Zootaxa* 1241: 1–36.

Dayan, T., Wool, D., and Simberloff, D. 2002. Variation and covariation of skulls and teeth: modern carnivores and the interpretation of fossil mammals. *Paleobiology* 28: 508–526.

Ferguson, C. A., Tucker, A. S., Christensen, L., Lau, A. L., Matzuk, M. M., and Sharpe, P. T. 1998. Activin is an essential mesenchymal signal in tooth development that is required for patterning of the murine dentition. *Genes Dev.* 12: 2636–2649.

Gingerich, P. D., and Schoeninger, M. J. 1979. Patterns of tooth size variability in the dentition of primates. *Am. J. Phy. Anthropol.* 51: 457–466.

Kangas, A. T., Evans, A. R., Thesleff, I., and Jernvall, J. 2004. Nonindependence of mammalian dental characters. *Nature* 432: 211–214.

Kavanagh, K. D., Evans, A. R., and Jernvall, J. 2007. Predicting evolutionary patterns of mammalian teeth from development. *Nature* 449: 427–432.

Kemp, T. S. 1982. *Mammal-Like Reptiles and the Origin of Mammals*. Academic Press, London, 363pp.

Klingenberg, C. P. 1996. Multivariate allometry. In L. F. Marcus, M. Corti, A. Loy, G. J. P. Naylor, and D. E. Slice (eds.). *Advances in Morphometrics*. Plenum Press, New York, pp. 23–49.

Klingenberg, C. P. 2008. Morphological integration and developmental modularity. *Ann. Rev. Ecol., Evol., Syst.* 39: 115–132.

Kuhl, F. P., and Giardina, C. R. 1982. Elliptic Fourier features of a closed contour. *Comput. Graph. Image Process.* 18: 259–278.

Kurtén, B. 1967. Some quantitative approaches to dental microevolution. *J. Dent. Res.* 46: 817–828.

Lazzari, V., Tafforeau, P., Aguilar, J.-P., and Michaux, J. 2008b. Topographic maps applied to comparative molar morphology: the case of murine and cricetine dental plans (Rodentia, Muroidea). *Paleobiology* 34: 46–64.

Lecompte, E., Aplin, K., Denys, C., Catzeflis, F., Chades, M., and Chevret, P. 2008. Phylogeny and biogeography of African Murinae based on mitochondrial and nuclear gene sequences, with a new tribal classification of the subfamily. *BMC Evol. Biol.* 8: 199. doi: 10.1186/1471-2148-8-199

Le Louarn, H., and Quéré, J.-P. 2003. *Les Rongeurs de France: Faunistique et Biologie*. INRA éditions, p. 256.

Michaux, J., Cucchi, T., Renaud, S., Garcia-Talavera, F., and Hutterer, R. 2007. Evolution of an invasive rodent on an archipelago as revealed by molar shape analysis: the house mouse in the Canary islands. *J. Biogeogr.* 34: 1412–1425.

Misonne, X. 1969. *African and Indo-Australian Muridae. Evolutionary trends*. Musée Royal de l'Afrique Centrale, Tervuren, Belgique, 219pp.

Mustonen, T., et al. 2003. Stimulation of ectodermal organ development by Ectodysplasin-A1. *Dev. Biol.* 259: 123–136.

Natsume, A., Koyasu, K., Oda, S.-I., Nakagaki, H., Kawai, T., and Hanamura, H. 2008. Tooth size variability and relevance of numerical variation in the Japanese serow. *Arch. Oral Biol.* 53: 95–98.

Olson, E., and Miller, R. 1958. *Morphological integration*. University Chicago Press, Chicago.

Penttilä, E., and Jernvall, J. 2008. Ectodysplasin in molar morphogenesis: graduality of signalling and patterning. Euro Evo Devo, *2nd Meeting of the European Society for Evolutionary Developmental Biology*, 265pp. (abstract with program).

Polly, P. D. 1998. Variability in mammalian dentitions: size-related bias in the coefficient of variation. *Biol. J. Linnean Soc.* 64: 83–99.

Prevosti, F. J., and Lamas, L. 2006. Variation of cranial and dental measurements and dental correlations in the pampean fox (*Dusicyon gymnocercus*). *J. Zool.* 270: 636–649.

Qiu, M., et al. 1997. Role of the Dlx homeobox genes in proximodistal patterning of the branchial arches: mutations of Dlx-1, Dlx-2, and Dlx-1 and -2 alter morphogenesis of proximal skeletal and soft tissue structures derived from the first and second arches. *Dev. Biol.* 185: 165–184.

Renaud, S. 2005. First upper molar and mandible shape of wood mice (*Apodemus sylvaticus*) from northern Germany: ageing, habitat and insularity. *Mamm. Biol.* 70: 157–170.

Renaud, S., Michaux, J., Jaeger, J.-J., and Auffray, J.-C. 1996. Fourier analysis applied to *Stephanomys* (Rodentia, Muridae) molars: nonprogressive evolutionary pattern in a gradual lineage. *Paleobiology* 22: 255–265.

Renaud, S., and van Dam, J. 2002. Influence of biotic and abiotic environment on dental size and shape evolution in a Late Miocene lineage of murine rodents (Teruel Basin, Spain). *Palaeogeogr., Palaeoclimatol., Palaeoecol.* 184: 163–175.

Renaud, S., and Michaux, J. R. 2003. Adaptive latitudinal trends in the mandible shape of *Apodemus* wood mice. *J. Biogeogr.* 30: 1617–1628.

Renaud, S., and Michaux, J. 2004. Parallel evolution in molar outline of murine rodents: the case of the extinct *Malpaisomys insularis* (Eastern Canary Islands). *Zool. J. Linnean Soc.* 142: 555–572.

Renaud, S., Auffray, J.-C., and Michaux, J. 2006. Conserved phenotypic variation patterns, evolution along lines of least resistance, and departure due to selection in fossil rodents. *Evolution* 60: 1701–1717.

Renaud, S., and Michaux, J. R. 2007. Mandibles and molars of the wood mouse, *Apodemus sylvaticus* (L.): integrated latitudinal signal and mosaic insular evolution. *J. Biogeogr.* 34: 339–355.

Rohlf, F. J. 2007. NTSYSpc, Numerical Taxonomy System, Version 2.2. Exeter Software, New York.

Rohlf, F. J., and Corti, M. 2000. Use of two-block partial least-squares to study covariation in shape. *Syst. Biol.* 49: 740–753.

Schluter, D. 1996. Adaptive radiation along genetic lines of least resistance. *Evolution* 50: 1766–1774.

Shimizu, T., Oikawa, H., Han, J., Kurose, E., and Maeda, T. 2004. Genetic analysis of crown size in the first molars using SMXA recombinant inbred mouse strains. *J. Dent. Res.* 83: 45–49.

Steiner, H. M. 1967. Untersuchungen über die Variabilität und Bionomie der Gattung *Apodemus* (Muridae, Mammalia) der Donau-Auen von Stockerau (Niederösterreich). *Zeitschrift für wissentschaftliche Zoologie* 177: 1–96.

Szuma, E. 2000. Variation and correlation patterns in the dentition of the red fox from Poland. *Ann. Zool. Fennici* 37: 113–127.

Tucker, A., and Sharpe, P. 2004. The cutting-edge of mammalian development; how the embryo makes teeth. *Nat. Rev. Genet.* 5: 499–508.

Van Valen, L. 1970. An analysis of developmental fields. *Dev. Biol.* 23: 456–477.

Wang, Y. J., Bleflower, R. M., Dong, Y.-F., Schwarz, E. M., O'Keefe, R., and Drissi, H. 2005. Runx1/AML1/Cbfa2 Mediates Onset of Mesenchymal Cell Differentiation Toward Chondrogenesis. *J. Bone Min. Res.* 20: 1624–1636.

Zhang, Y. D., Chen, Z., Song, Y. Q., Liu, C., and Chen, Y. P. 2005. Making a tooth:growth factors, transcription factors, and stem cells. *Cell Research* 15: 301–316.